Technical Note BN-467 August, 1966

SHOCK TUBE SPECTROSCOPY AT CHROMOSPHERIC TEMPERATURES*

by

T. D. Wilkerson for the

Atomic Radiation Group**

* Report of research progress on NsG-359
during period October, 1965 - July, 1966

**G. Charatis, D. W. Koopman, T. D. Wilkerson (faculty)
R. Bengston, T. LaSalle, M. Miller, P. Murphy (res. grad. assts.)
S. McPhillips, G. Monahan, R. Roig, S. Cameron (assistants)

* This work was supported in part by the Contract NsG 359 with the National Aeronautics Space Administration

SHOCK TUBE SPECTROSCOPY

AT CHROMOSPHERIC TEMPERATURES

Abstract

Results of recent spectroscopic experiments with a gas-driven shock tube are described, including technical developments, progress in redundant measurements of plasma state, and data on atomic line strengths for neutral carbon.

1. Introduction

In company with other research groups in "experimental astrophysics", we believe that thermal light sources should continue to be used and improved for line-strength measurements. Other methods, used increasingly in recent years, do not depend on thermal excitation relations; however, they require unambiguous interpretation of radiative decay times (or distance) or excitation-radiation phase lags. Because of difficulties in both the thermal and non-thermal methods, the two approaches often show comparable accuracies. Both will remain important for many years, in order that systematic errors may be avoided.

In the past few months, the thermal light source of interest to us -- namely a 3" x 4" gas-driven shock tube -- has been studied by several diagnostic procedures which are still being refined. The general result is that data on line strengths of light elements are accessible through the observational techniques and the methods of data reduction we have used. For the lighter elements and their ions, temperatures of $10{,}000^{\circ}$ K and upward must usually be employed. The general philosophy is to determine atomic line strengths using as many redundant measurements as possible on the thermodynamic variables such as temperature, pressure and number density of electrons. While our work goes ahead to other elements and to more thorough measurements on carbon, we want to report here the carbon results recently obtained, the spectroscopic methods yielding the current level of precision, and some of the operating techniques now adopted for this work.

In what follows, we will assume the reader is familiar with certain salient features of shock tube operation:

(a) The incident and reflected shock waves compress a gas sample of known composition, so that its pressure is a few hundred times (and the temperature several tens of times) the initial value. Typically we obtain: pressure $\sim$ 6 atmos., temperature $\sim$ 11,000° K behind reflected shocks in such mixtures as 99.5% neon plus 0.5% methane (CH_4).

(b) The thermal state of this gas can, in principle, be calculated from the initial composition, pressure and temperature and the incident shock velocity -- assuming non-dissipative, one-dimensional flow and the conservation relations appropriate thereto. In fact, dissipative departures from this "ideal flow" are often seen which are of order 10-20%. In order, therefore, to avail oneself of the very attractive degree of heating in shock waves, precise measurements of thermal (and radiative) state are required.

(c) Any shock tube state lasts only a short time in ordinary terms, due to the high shock velocities necessary for generating high temperatures and reasonable limits on apparatus size. Our times are of order 50-100 microseconds behind the reflected shock, with a degree of transiency still present, so our aim is to collect data during 2-10 microsecond periods when steadiness can be assumed. Each shock tube "shot" is treated as a separate experiment, while the time-evolution within each shot allows a range of variables to be covered. The operating range for each shot is easily varied by changing the driving pressure or other initial conditions. Accuracy of composition, line-of-sight uniformity and plenty of time for equilibration are all points in favor of the gas-driven shock tube as a spectroscopic source.

(d) Atomic line strengths are deduced from measured line intensities (emission or absorption) coupled to knowledge of abundance of the species (e.g.; carbon in the CH_4 - neon shots) and the related ionization-excitation equilibria (e.g., the Boltzmann factor for the upper or lower level of the line in question). Accuracy of all the thermal methods is therefore determined by the accuracies with which line-intensity and level population are known. For a high-excitation line of a given element, a temperature error can be magnified by the ratio of level energy to temperature, unless more than the bare minimum of types of observation is made. Complementary, even redundant, measurements are called for.

Section 2 treats calculations of shock tube states, both from the Rankine-Hugoniot point of view (based on incident shock velocity) and from the more general specification of the variables p, T (pressure and temperature) which tacitly assumes they will be measured; for measurements see Sections 3 and 4. Section 5 discusses a sequential image dissector and its use in measuring electron densities. Line strengths for visible carbon lines are given in Section 6, and directions of current research are indicated in Section 7.

2. Calculation* of Thermodynamic States and Shock Conditions (Koopman)

Two types of machine calculations have been developed and are employed in reduction and analysis of experimental data: (a) calculation of the degrees of ionization and excitation of the various atomic and ionic species, where two thermodynamic variables ($T\text{-}N_{total}$, $T\text{-}N_e$, T-p, etc.) and initial molecular composition are known quantities and (b) calculation of the thermal state and of the atomic and ionic abundances and excitation populations, in both the primary and reflected shock regions, as a function of initial shock speed and gas composition.

As the experimental apparatus has been developed to yield accurate measurements of the plasma state directly, calculations of type (a) are employed as the primary means of reducing measured optical intensities to yield f-values, while the shock calculations (b) are used to calculate the conditions expected on the basis of the measured shock speed and to predict the results of proposed

---

*Computing services were provided by the University of Maryland Computer Science Center.

studies. The agreement between predicted and measured shock conditions will form the basis for other studies, primarily to see whether discrepancies arise from hydrodynamic imperfections or some more interesting phenomena.

The present calculations are continuations of earlier treatments of high temperature equilibrium and shock phenomena;[1,2] the solution of the problem of simultaneous multiple ionization processes for a mixture of elements is based on a published iterative procedure which has been modified for more rapid convergence.[3] Solutions of the shock equations for a real gas are based on a graphical technique which has been developed to include kinetic, dissociative and ionizational energy terms calculated on an atomic basis, and has been interpreted in an algebraic form for numerical iteration.[4] A detailed calculation of atomic and ionic partition functions, lowered ionization potentials, and a consideration of neutral, single and double ionized species are included in the analysis. Both types of calculations have been coded in the Michigan Algorithm Decoder (MAD) language; current programs will solve for initial mixtures of neon plus the additives H_2, Ar, N_2, O_2, CH_4, H_2S and CS_2 in arbitrary concentrations. The programs can readily be expanded to include a wider range of additives.

Figure 1 is an example of the application of the type (a) calculation, yielding number densities for various species in a plasma of fixed composition and total number density as a function of temperature; Figure 2 demonstrates the results obtained from the type (b) calculation, where shock conditions as well as number densities are predicted as a function of shock speed.

3. Temperature Measurements via Line Reversal and Absolute Line Intensity (Charatis)

Of several methods employed for temperature measurement, two are described and compared here. Both are made simultaneously with the same Bausch and Lomb spectrograph (f/18) viewing the shock tube perpendicular to the flow axis. The spectrograph is used as a polychromator with three pairs of channels located at the Balmer line H_α (λ6563), a strong NeI line (λ5852), a C I line (λ5052) and their nearby, line-free continua. The channels are constructed similarly to the elements of the multi-channel "squid" discussed in Section 5 below; i.e. glass cover slides joined to fibre bundles which carry light to photomultipliers. All channels are absolutely calibrated with a carbon arc anode, [5,6] care being taken that the illumination of the optic elements is always the same. The recording of all channels is made on triggered oscilloscope sweeps; triggering is derived from pressure transducers in the shock tube, so that light from all flow regions can be observed.

(a) Line Reversal temperatures are measured primarily with the H_α channels, since the relatively high optical depth of this line lends great sensitivity to the method. The flash lamp which shines through the shock tube has been described elsewhere,[7] and a more recent article on this type of discharge[8] will prove useful to the interested reader. The flash lamp discharge is usually triggered about 35 microseconds after the time (t_o) when the first reflected shockwave crosses the optic axis. Peak brightness temperature of the lamp is typically 22,000° K in the visible spectrum,

and absorption by the cooler gas in the shock tube is quite evident on those channels centered on strong lines.

We first tried to measure NeI line reversal directly,[9] encountering low precision due to low optical depth, and have since concentrated on H_α for best results. Currently the precision in specifying the "cross over" between emission and absorption spectra is about 1%.

Reversal temperatures for H_α are compared to Rankine-Hugoniot predictions in part (a) of Figure 3. Since the dashed line represents identical temperatures, the reversal values are about 10% higher than the ideal prediction when the latter is near 10,000° K. Agreement within the expected errors is observed from 12,000 to 13,000°K. The error attached to the predicted temperature arises from fluctuations in the timing circuitry used to measure primary shock speed. All spectral lines (H_α , NeI, C I) demonstrate a 2% rise in temperature between t_o and t_o + 35 μsec, so some disparity between the reversal and predicted values is not surprising. That both the temperature and pressure show noticeable increases behind the reflected shock wave indicates that the shock tube flow departs somewhat from the constancy one assumes in Rankine-Hugoniot calculations.

The H_α reversal data show that the population ratio of the n = 3 and n = 2 levels of neutral hydrogen is given by a temperature which roughly agrees with hydrodynamic expectations and which can be determined with precisions of order 200 - 300° K.

(b) Absolute line intensity measurements, utilizing lines of known oscillator strength, settle the question of whether the energy levels of the element in question are populated according to the same temperature one deduces from hydrogen line-reversal.

This is a demanding check on local thermal equilibrium, if one uses an element such as neon for which the abundance and energy level spacings are quite different than for the hydrogen. For NeI, many line strengths now seem well known from a series of measurements using thermal sources and, in later years, radiative lifetime techniques. From the recent National Bureau of Standards compilation,[10] we adopted the value $A = 0.75 \times 10^{8}$ sec $^{-1}$ for NeI λ5852.49. Since the accuracy of this value is of order 10%, the line is suitable for temperature determinations to a precision of order 1%.

The density of neutral neon atoms in the ground state was determined for each experiment by means of the p, T program (Section 2) together with measured pressures (Section 4) and reversal temperatures (above). Though it might seem circular, therefore, to compare the final NeI temperatures with reversal temperatures, it is easily shown that this is not the case. In this method, the reversal temperature appears multiplicatively in front of the Boltzmann factor one is trying to determine - and not within the exponential where it would confuse the issue.

Using densities inferred in this manner and the transition probability for NeI given above, Boltzmann factors - and therefore excitation temperatures - were found for the upper neon level which lies nearly 19 eV above the ground state. The results are shown in part (b) of Figure 3, compared with reversal temperatures measured for the same plasmas. The two methods are in good agreement over the temperature range studied (10,500 - 11,500° K).

Thus, measurements on the relative level populations of

one atomic species and the absolute level populations of another yield the same temperature, and give strong support to assumptions of local thermal equilibrium in further experiments with this shock tube plasma.

4. Pressure and Shock Velocity Measurements with Quartz Transducers (Murphy)

Oscilloscopic records of pressure histories are made at two shock tube positions by means of the Kistler quartz guage (Model 601A) and charge amplifier (Model 568). For the experiments culminating in the data given in Section 6, two transducer-amplifier stations were located in the top wall of the shock tube. One was close to the spectroscopic line of sight, so that we could (a) record the absolute pressure behind the reflected shock appropriate for spectroscopic data reduction, and (b) observe the times-of-arrival of both the incident and reflected shock waves. The other transducer was 20 cm further upstream where the arrival of the incident shock was the principal observable, so that the velocity of that shock could be determined on a 60 microsecond time-base.

Delay circuits were employed to get both pressure histories on the same CRO picture with good time resolution. We encountered timing fluctuations of order 1.0 - 1.5 microsecond which rendered the shock velocity measurements imprecise to a level of 2%. This is the source of the 4% uncertainty in temperature as calculated from the Rankine-Hugoniot equations (Section 3a and Figure 3a). Further work is under way to reduce these fluctuations and to insure that no systematic error is introduced by converting one pressure

rise into an electronic trigger pulse while using the other pressure trace in its fully displayed form.*

Absolute pressures, measured behind the reflected shock wave, provide the companion data to reversal temperatures, in order that the thermal state of the gas is completely specified at the time when atomic line intensities are being observed photoelectrically and photographically. The pressure transducers were calibrated by the manufacturer. A re-calibration by us, using a dead-weight tester, agreed with the manufacturer's calibration to 1.5%. The net precision of shock tube pressure measurements is 4% - 5%. The pressure and temperature data are the inputs for the (p,T) program (Section 2), while pressures themselves (at t_o + 35μsec) are 25% higher than the Rankine-Hugoniot predictions. This comparison describes the majority of shots which were made with initial pressures of 10 Torr (neon plus 0.5% CH_4). For the few shots at 14 Torr and above, the agreement is much closer. The pressure ratio immediately across the reflected shock scatters between 6 and 8, which is to be compared to the theoretical limit of 6 for strong shocks in permanent gases having three translational degrees of freedom. As well as demonstrating a shot-to-shot scatter, the pressure histories show a steady rise behind every reflected shock, providing further evidence for a degree of transiency in the incident flow field. Experience indicates that

---

*At a third shock tube station, upstream of both transducers, a resistive film-strip plug has been installed in the side wall, enabling us to display the full wave forms from both transducers on the same CRO picture.

the reproducibility and uniformity will be improved by the use of more rapidly opening shock tube diaphragms.

As well as directly providing the values of pressure needed for thermodynamic and spectroscopic analysis, the quartz transducers confirm that the shock tube pressures fall approximately in the range expected from simple theory. This range is 5 - 10 atmospheres in our case.

5. Line Profile and Electron Density Measurements (Miller)

Balmer line profiles (principally H_β) are observed photoelectrically and photographically, in order to determine electron density in the shock tube plasma. This provides another check on (p,T) calculations, namely the accumulated effects of all ionization reactions. Similar techniques will be applied to other lines, so that existing calculations of Stark broadening can be checked for several elements.

(a) Photoelectric Measurements - A sequential image disector[9] ("squid") has been refined to the point that it can be routinely used with the shock tube. The principle of this device is shown in Figure 4, where we have indicated a wide H_β profile being segmented by a squid placed in the image plane of a spectrograph. We have reported the ultraviolet extension of this technique by means of a sodium salicylate coating.[12] The principal element is a microscopic cover slide, overcoated with MgF_2 and aluminum to prevent cross-talk between channels, and joined onto an optical fibre bundle which carries light to a photomultiplier. The Appendix contains the abstract of reference 12, wherein features of the image-

dissection method are given and compared to other methods for photoelectric recording of line profiles.

Currently a twelve-channel squid dissects H_β into 1 Å-wide segments, each of which is recorded on a precalibrated oscilloscope channel. This arrangement provides continuous recording in all wavelength bands with a time resolution of order 1 microsecond. Figure 6 shows several H_β profiles reduced from one shock tube experiment, including the unfolding of the monochromator slit function. Also shown are theoretical profiles from Griem, Kolb and Shen,[13] chosen for the best fits to the data, and the corresponding electron densities which we determine with 10% precision by this method. The electron density at t_o + 42 microseconds agrees to within 10% with the electron density calculated from the (p,T) program and the observed pressure and temperature at that time.

Two stages of improvement for the "squid technique" are (i) computer reduction of data of the present type, using a stored tabulation of theoretical calculations,[13] and (ii) magnetic tape recording of the squid channels for direct computer input. The program for stage (i) is being written. Stage (ii) awaits the necessary funding for a tape recorder of the telemetry type.

(b) Photographic Measurements: For the experiments discussed in Section 6, H_β profiles were photographically recorded on the same calibrated films as were used for carbon lines. Electron densities were again obtained from the half-width of H_β, following the reduction of photographic density to intensity and the unfolding of the spectrograph slit function. The electron densities so measured agreed with those calculated from

the (p,T) program, to within the measurement precision of 10 - 15% which varied with film quality. The "squid technique" was not applied in this particular set of measurements because of breakdowns in some of the requisite oscilloscope channels. Future data runs will employ both techniques simultaneously until we fully verify that the multichannel, photoelectric observations are sufficient by themselves for measuring electron density over suitably wide ranges of electron density and light intensity. Continued applications of both methods together may allow us to improve the precision of electron density measurements to 5%.

Predicted electron densities in the range $1 - 5 \times 10^{16}$ per cc have therefore been verified to a precision of order 10%, by means of photoelectric and photographic records of the Balmer line H_β. Thus we have further evidence for good understanding of the shock tube plasma; in particular, what one might call the "ionization temperature" (assuming zero error in pressure determinations) is within 2% of temperatures determined by other means.

6. Absolute Transition Probabilities for Lines of Neutral Carbon (Wilkerson)

A series of experiments has been run to determine the absolute transition probabilities for lines of neutral carbon between 4600 and 5400Å. The shock tube plasma was observed by most of the methods described in foregoing sections, and the data reduced with the aid of (p,T) programs. CI λ5052 was recorded photoelectrically in the manner given at the beginning of Section 3, and other carbon line intensities (relative to λ5052) were measured with the moving

film spectrograph alluded to in Section 5 (Jarrell-Ash, f/6.3) illuminated by means of a Bausch and Lomb fibre optic bundle.

Absolute line intensities (photoelectric) for CI λ5052 were reduced to absolute transition probabilities by calculating the appropriate number of carbon atoms in the line of sight *via* the (p,T) program and measured pressures and temperatures; the result is:

$$A\ (CI\ \lambda 5052) = 0.026 \pm .007\ (27\%) \times 10^{8}\ sec^{-1}$$

Relative intensities for other lines relative to λ5052 were measured photographically with a precision of 20%; compounding both errors in these lines leads then to a precision of 34% in absolute value. All our results for this transition array are summarized in Figure 6, where our shock tube values are plotted against the 50% estimates made by Wiese *et al*[10] from previous studies of these lines.

In effect, then, we find the same pattern of relative transition probabilities within this array, in agreement with LS coupling, but arrive at a somewhat higher absolute value. Our absolute value for λ5052, for example, is double that of Richter[14], five-eighths that of Doherty[15] and 1.5 times that of Wiese *et al*. Of course, the precisions are not yet so good as to choose between different radial matrix elements for this transition array; our present line of work is to (a) improve the precision of our mixing and intensity measurement procedures and (b) to vary the shock tube conditions and add to the complement of data-taking procedures, so as to avoid systematic errors.

7. Conclusions

A set of direct measurements of the state of the shock tube plasma has yielded absolute transition probabilities for several lines of neutral carbon. No inconsistencies were found in the diagnostic measurements, and the relative line strengths agree with LS coupling for the transition array under study. Absolute line strengths are higher than most of the prior determinations, but significantly less than an earlier shock tube result.

Improved line strength measurements are coming out of present diagnostic procedures which include several more independent determinations of temperature and a more precise measurement of electron density. Absolute transition probabilities are being remeasured for carbon, and new values measured for sulphur. Exploratory films are being taken for lines of the rare gases and the halogens. Completion of some of this work must await the laboratory's relocation in the Space Sciences Building, a new facility provided by NASA on the College Park campus. We expect that continued use of the shock tube in the manner we have described will yield copious data of interest in atomic physics and astrophysics alike.

REFERENCES

1. D. W. Koopman, "Performance Studies and Ne II Line Strength Measurements with an Electrically Driven Shock Tube", Ph.D. thesis, University of Michigan (1963).

2. D. W. Koopman, Phys. Fluids 7, 1651 (1964).

3. C. A. Rouse, Astrophys, J. 134, 435 (1961); 135, 599 (1962); 136, 636 (1963).

4. G. H. Markstein, Am. Rocket Soc. J. 29, 588 (1959).

5. J. Euler, Ann. Physik 14, 145 (1954); 18, 345 (1956).

6. M. R. Null and W. W. Lozier, Jour. Opt. Soc. Am. 52, 1156 (1962).

7. G. Charatis and T. L. Hershey, "A Flash-Lamp Source of High Intensity Continuous Spectra", University of Maryland Technical Note BN-361 (July 1964).

8. J. E. G. Wheaton, Applied Optics 3, 1247 (1964).

9. T. D. Wilkerson, "Atomic Processes in Plasmas" in Proceedings of the Symposium on Dynamics of Fluids and Plasmas (October 1965) Academic Press, in press.

10. W. L. Wiese, M. W. Smith, and B. M. Glennon, Atomic Transition Probabilities, Volume 1: Hydrogen through Neon , National Standard Reference Data Series - National Bureau of Standards 4 (May 1966).

11. H. R. Griem, Phys. Rev. 128, 515 (1962); also H. R. Griem Plasma Spectroscopy, McGraw-Hill (1964).

12. M. H. Miller, T. D. Wilkerson and J. R. W. Hunter, Proceedings of the Culham Conference on UV and X-Ray Spectroscopy of Plasmas , Institute of Physics, London (1966).

13. H. R. Griem, A. C. Kolb and K. Y. Shen, Astrophys J. 135, 272 (1962).

14. J. Richter, Z. Physik 151, 114 (1958).

15. L. R. Doherty "The Measurement of Absolute Spectral Line Strengths with the Shock Tube", University of Michigan Ph.D. Thesis (1952).

FIGURE CAPTIONS

Figure 1. Number density of species as a function of temperature for a quasi-equilibrium plasma initially composed of neon plus 0.2% CH_4, at a total atomic number density of $3.7 \times 10^{18}/cm^3$.

Figure 2. Temperature, pressure, and species density calculated for reflected shock region as a function of initial shock speed. Initial gas conditions: $T_o = 300^o$ K, $p_o = 10$ torr, composed of neon plus 0.25% CH_4.

Figure 3 Comparisons of temperatures for reflected shock region. (a) T as obtained from line reversal measurement 35μsec after passage of reflected shock vs. T immediately behind reflected shock as calculated from measured shock speed; (b) reversal temperature at 35μsec vs. T at 35μsec obtained from absolute NeI line intensity (λ5852 Å).

Figure 4. Sequential image dissector (squid) for precise partition of spectral line profiles into narrow wavelength bands. Particular use for H_β profiles is indicated schematically.

Figure 5. Several H_β profiles in one experiment, reduced from squid data recorded as functions of time. Theoretical profiles and electron densities according to Griem, Kolb Shen (ref. 13).

Figure 6. Neutral carbon transition probabilities (shock tube) compared with compilation of previous work.

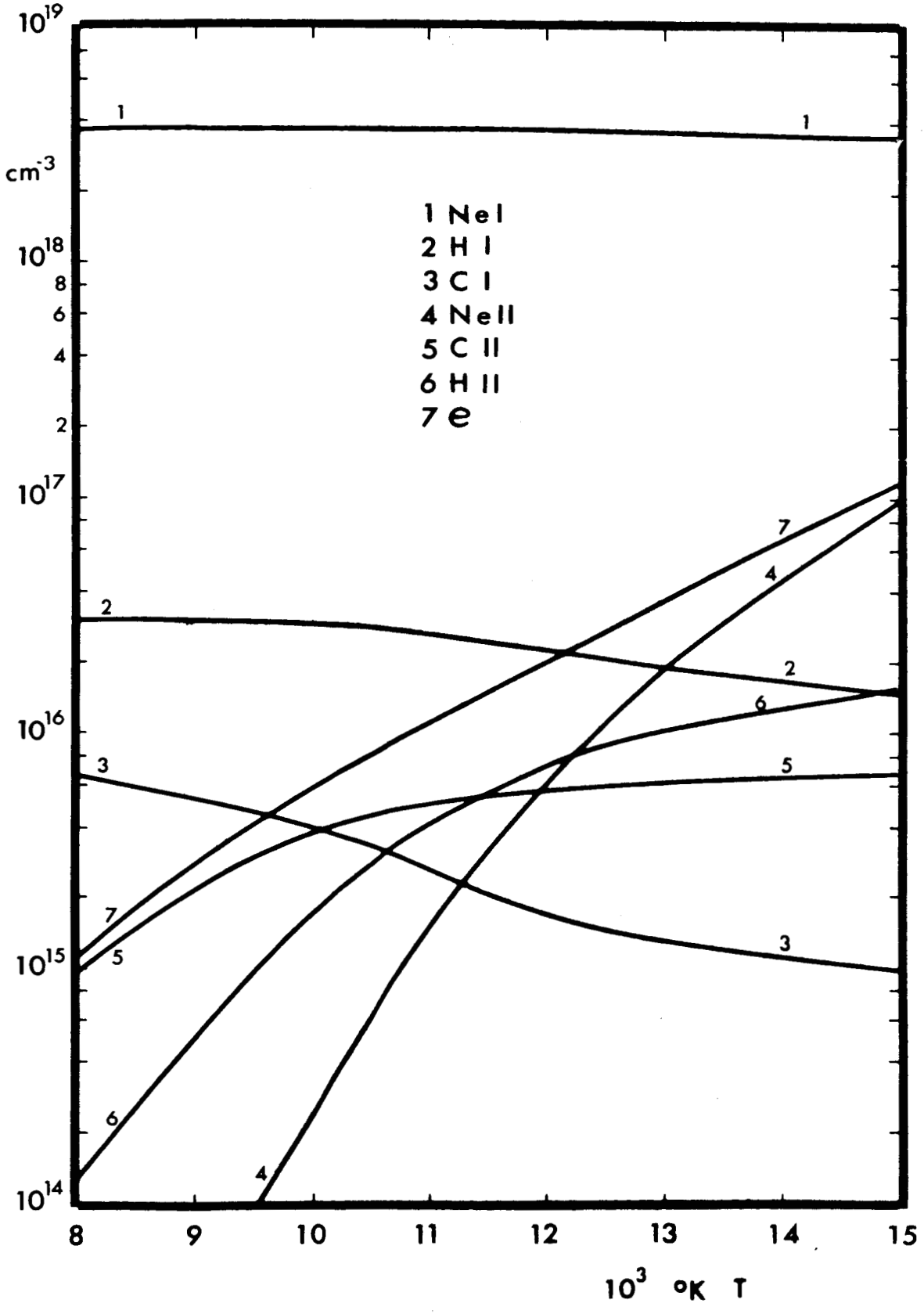

FIGURE 1

R. Lucano
'85

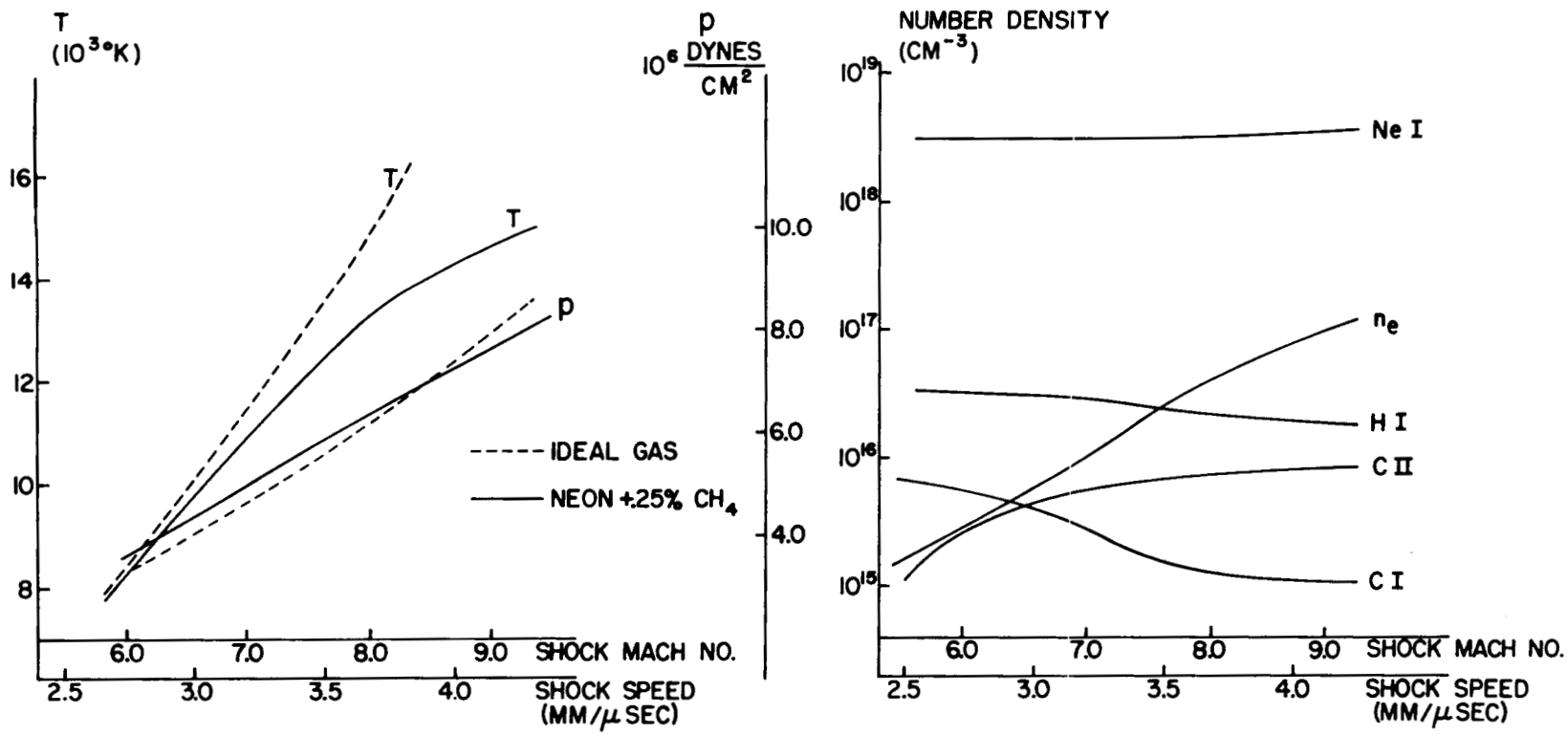
T
(10³°K)
16
14
12
10
8
T
T
p
p
10⁶ DYNES/CM²
10.0
8.0
6.0
4.0
IDEAL GAS
NEON +.25% CH₄
6.0
7.0
8.0
9.0
SHOCK MACH NO.
2.5
3.0
3.5
4.0
SHOCK SPEED
(MM/μSEC)
NUMBER DENSITY
(CM⁻³)
10¹⁹
10¹⁸
10¹⁷
10¹⁶
10¹⁵
Ne I
nₑ
H I
C II
C I
6.0
7.0
8.0
9.0
SHOCK MACH NO.
2.5
3.0
3.5
4.0
SHOCK SPEED
(MM/μSEC)

FIGURE 2

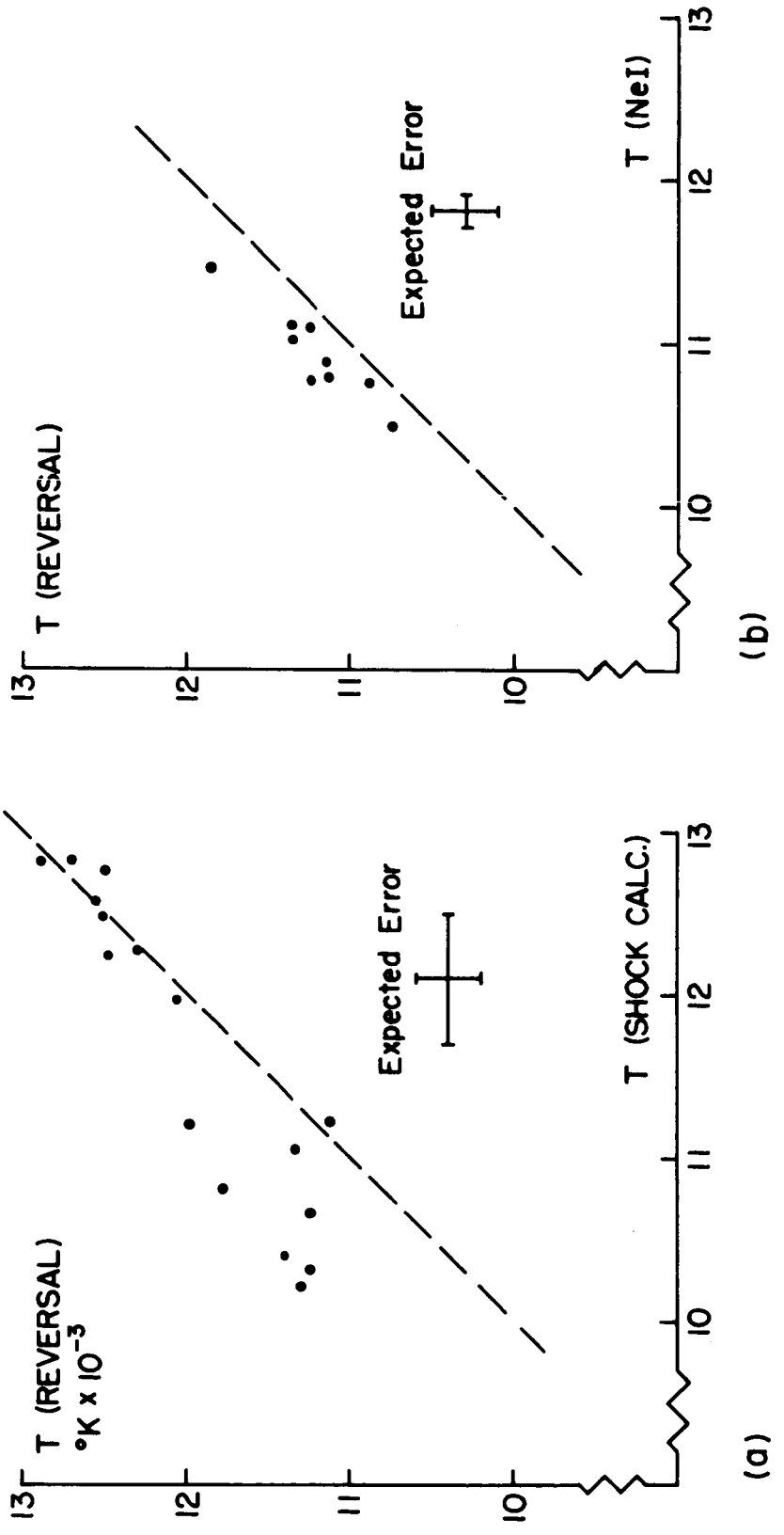
T (REVERSAL)
°K x 10⁻³
13
12
11
10
Expected Error
T (SHOCK CALC.)
10
11
12
13
(a)
T (REVERSAL)
13
12
11
10
Expected Error
T (NeI)
10
11
12
13
(b)

FIGURE 3

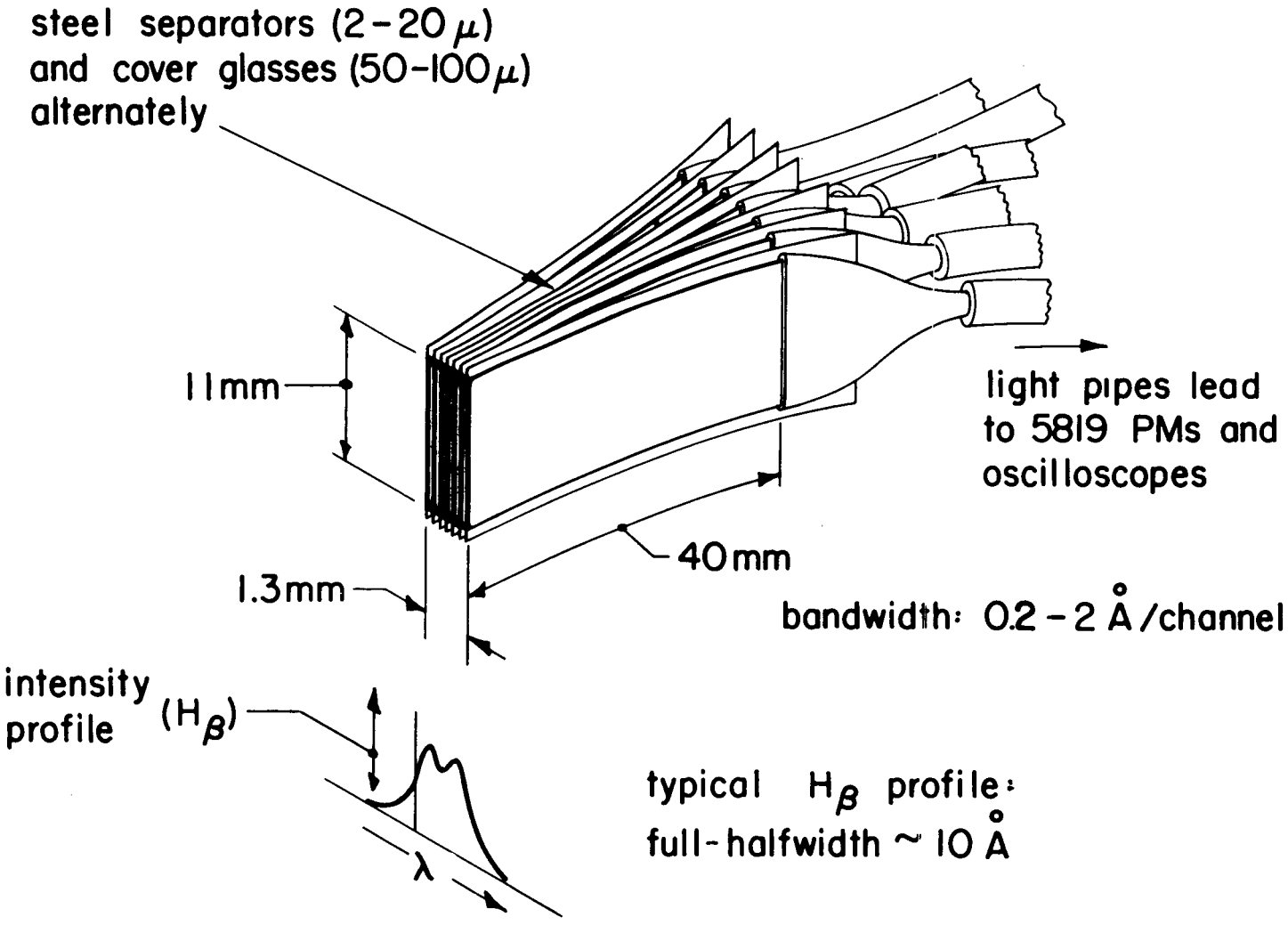
steel separators (2-20 μ)
and cover glasses (50-100 μ)
alternately
11mm
light pipes lead
to 5819 PMs and
oscilloscopes
40mm
1.3mm
bandwidth: 0.2 - 2 Å/channel
intensity
profile
(Hβ)
λ
typical Hβ profile:
full-halfwidth ~ 10 Å

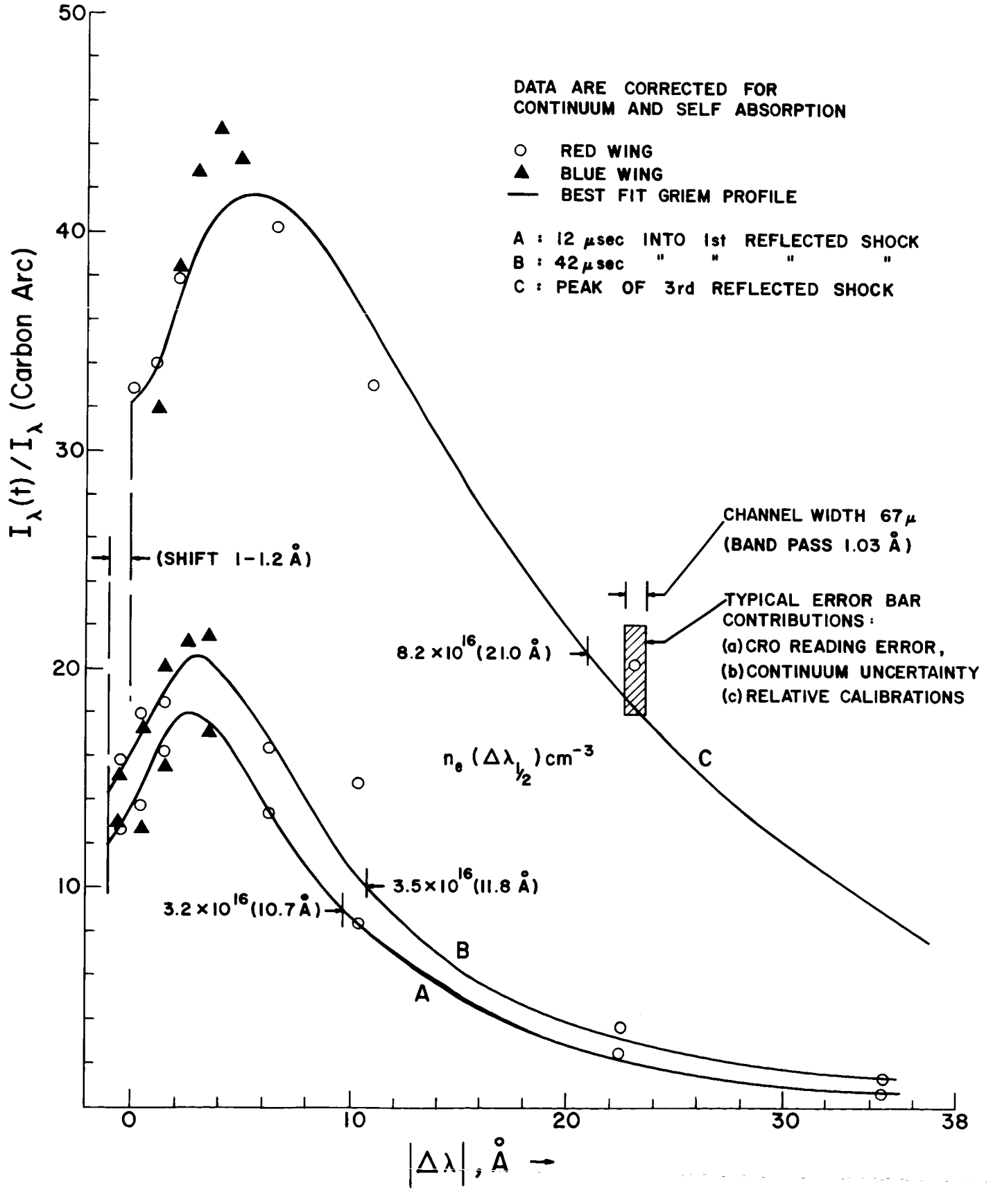
H_β PROFILES SAMPLED SUCCESSIVELY BY 12-CHANNEL SQUID
DATA ARE CORRECTED FOR CONTINUUM AND SELF ABSORPTION
○ RED WING
▲ BLUE WING
— BEST FIT GRIEM PROFILE
A : 12 μsec INTO 1st REFLECTED SHOCK
B : 42 μsec " " " "
C : PEAK OF 3rd REFLECTED SHOCK
$I_\lambda(t) / I_\lambda$ (Carbon Arc)
(SHIFT 1-1.2 Å)
CHANNEL WIDTH 67 μ
(BAND PASS 1.03 Å)
TYPICAL ERROR BAR CONTRIBUTIONS:
(a) CRO READING ERROR,
(b) CONTINUUM UNCERTAINTY
(c) RELATIVE CALIBRATIONS
8.2×10^{16} (21.0 Å)
$n_e (\Delta\lambda_{1/2})$ cm^{-3}
3.5×10^{16} (11.8 Å)
3.2×10^{16} (10.7 Å)
A
B
C
50
40
30
20
10
0
10
20
30
38
$|\Delta\lambda|$, Å

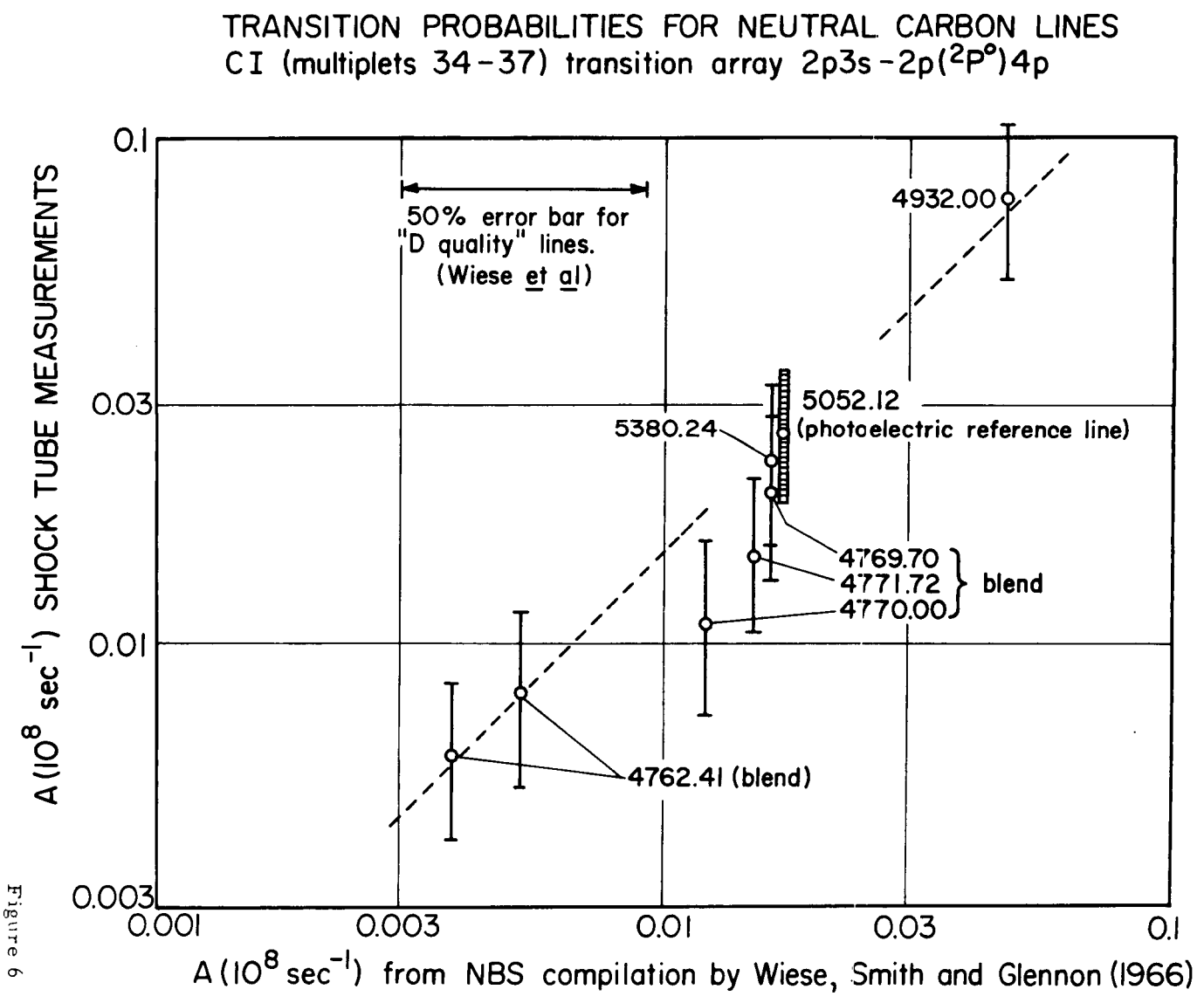
TRANSITION PROBABILITIES FOR NEUTRAL CARBON LINES
CI (multiplets 34-37) transition array 2p3s-2p(²P°)4p
50% error bar for "D quality" lines. (Wiese et al)
4932.00
5052.12
(photoelectric reference line)
5380.24
4769.70
4771.72
4770.00
blend
4762.41 (blend)
0.1
0.03
0.01
0.003
0.001
0.003
0.01
0.03
0.1
A (10⁸ sec⁻¹) SHOCK TUBE MEASUREMENTS
A (10⁸ sec⁻¹) from NBS compilation by Wiese, Smith and Glennon (1966)

Figure 6

APPENDIX (Summary, Reference 12)

PAPER 55: CULHAM CONFERENCE ON ULTRA-VIOLET AND X-RAY SPECTROSCOPY OF LABORATORY AND ASTROPHYSICAL PLASMAS
29 March - 1 April, 1966

Spectroscopic image dissector*
by M. H. Miller and T. D. Wilkerson (University of Maryland) and J. R. W. Hunter (University of Edinburgh).

A method of image dissection is described for photoelectric spectroscopy of plasmas which extends techniques previously used or suggested.[1] The method is easily and inexpensively applied, and is particularly useful for obtaining time-resolved line profiles and intensities in a single experiment. Compared to scanning spectrometers, the image dissector is generally advantageous for avoiding errors introduced by the signal having significant Fourier amplitudes near the scanning frequency. Multi-channel devices will become even more attractive for laboratory use as high frequency tape recorders become more available.

Our image dissectors are linear arrays of microscope coverglass slides in the thickness range 50-100 μ. Ten or more channels are easily incorporated in a single device (SQUID) which sits in the image plane of a spectrograph. Each channel conducts light in its bandpass (<1Å) to a separate photomultiplier and CRO. The channels are adjacent in wavelength or separated by spacers, crosstalk having been eliminated by 3-5 μ steel shims or by vacuum-deposited layers of flourides and aluminum. The choice of optical connection between each glass slide and its photomultiplier depends on whether ease of handling or transmissivity is the more important consideration. In the former case, ordinary fibre optics form the connection, giving overall efficiencies of 10% - 30%, depending on length (10-30 cm) and care in optically joining the fibre bundle with its glass slide and photomultiplier. In the latter case, long cover glasses (8-12 cm) which can support a 90° bend are directly bonded to small photomulti-

pliers in a close-packed array; efficiencies here are of order 60%-80%.

Most of our development has been in the visible, where we use a 12-channel squid having 0.8 Å resolution to record Stark-broadened H_β profiles emitted from a gas-driven shock tube. (T ~11,000-14,000°K; full halfwidth of H_β ~10-20 Å). Several inexpensive CROs record the line profile segments with microsecond time resolution during the 100μ sec period following shock reflection.

We have extended this technique into the ultraviolet by coating the ends of the cover glasses with sodium solicylate, rather than by using quartz slides as previously suggested.[1] Though the latter method may prove more efficient, the phosphor method offers wider spectral range, greater ease of fabrication and less expensive resolution. At 2537Å, glass slides simply end-coated with sodium salicylate gave signals roughly 30% - 80% of those obtained with equal apertures covering a sodium salicylate screen in front of the photomultiplier. Just as with ordinary phosphor assemblies, a squid device can be easily filtered for more selective response to vacuum ultra-violet radiation.[2]

* This research was supported in part by National Aeronautics and Space Administration Grant NsG-359

1. J. G. Hirschberg, Jour. Opt. Soc. Am. 53, 507 (1963); Report No. MATT-187, Princeton University (April 1963).

2. R. Lincke and T. D. Wilkerson, Bull. Am. Phys. Soc. 8, 165 (1963) R. Lincke and G. Palumbo, Jour. of Appl. Optics 4, 1677 (L) (1965).